

Critical exponents at the unconventional disorder-driven transition in a Weyl semimetal

S.V. Syzranov^{1,2}, P.M. Ostrovsky^{3,4}, V. Gurarie^{1,2}, L. Radzihovsky^{1,2,5}

¹*Physics Department, University of Colorado, Boulder, Colorado 80309, USA*

²*Center for Theory of Quantum Matter, University of Colorado, Boulder, Colorado 80309, USA*

³*Max Planck Institute for Solid State Research, Heisenbergstr. 1, 70569 Stuttgart, Germany*

⁴*L.D. Landau Institute for Theoretical Physics RAS, 119334 Moscow, Russia*

⁵*JILA, NIST, University of Colorado, Boulder, Colorado 80309, USA*

(Dated: March 6, 2022)

Disordered non-interacting systems in sufficiently high dimensions have been predicted to display a non-Anderson disorder-driven transition that manifests itself in the critical behaviour of the density of states and other physical observables. Recently the critical properties of this transition have been extensively studied for the specific case of Weyl semimetals by means of numerical and renormalisation-group approaches. Despite this, the values of the critical exponents at such a transition in a Weyl semimetal are currently under debate. We present an independent calculation of the critical exponents using a two-loop renormalisation-group approach for Weyl fermions in $2 - \varepsilon$ dimensions and resolve controversies currently existing in the literature.

PACS numbers: 72.15.Rn, 64.60.ae, 05.70.Fh, 72.10.Fk

It was proposed^{1,2} 30 years ago that three-dimensional (3D) disordered systems with Weyl and Dirac quasiparticle dispersion can display an unconventional disorder-driven transition that lies in a non-Anderson universality class. In particular, in contrast with the Anderson localisation transition, the density of states at this transition has been suggested¹ to display a critical behaviour, with the scaling function proposed in Ref. 3.

Recently we have demonstrated^{4,5} that such transitions occur near nodes and band edges in *all* materials in sufficiently *high dimensions* d and are not unique to Dirac (Weyl) systems. In systems that allow for localisation the transition manifests itself also in the unusual behaviour of the mobility threshold⁵. As the concept of high dimensions here is defined relative to the quasiparticle dispersion, possible playgrounds include a number of systems in physical $d = 1, 2, 3$ dimensions, with higher dimensions being accessible numerically. For example, recently we have shown how this transition can be observed in 1D and 2D arrays of ultracold ions in optical or magnetic traps⁶.

Because Weyl semimetals (WSMs) are currently one of the most well-known and experimentally accessible platforms^{7–9} for the observation of these high-dimensional disorder-driven phenomena, tremendous research efforts have been directed at studying the critical properties of the transition in a WSM. Nevertheless, the values of the critical exponents at the transition are currently under debate.

Quantum criticality near the transition has been studied analytically for Dirac and Weyl particles in dimensions $d > 2$ by means of perturbative renormalisation-group approaches^{10,4,5,11}, large- N (large number of valleys or particle flavours) analysis¹², and (uncontrolled) self-consistent Born approximation^{1,13,14} (SCBA), equivalent to a large- N calculation in the limit $N = \infty$.

Usually Weyl and Dirac materials have only several

nodes, $N \sim \mathcal{O}(1)$, which makes large- N approaches quantitatively inaccurate in all dimensions d [for detailed criticism of the SCBA vs. RG see Refs. 15,16, 4 (although Refs. 15 and 16 are devoted to graphene, their arguments apply as well to Dirac and Weyl particles in all dimensions)].

Perturbative renormalisation-group (RG) analysis are controlled by the small parameter $\varepsilon = 2 - d$. Although such RG analysis for small ε is not guaranteed to be quantitatively accurate when analytically continued to 3D ($\varepsilon = -1$), already the one-loop results^{10,4,5,11} predict the correlation-length exponent $\nu = 1$ and the dynamical exponent $z = 3/2$ that lie within 15% and several percent of the values obtained numerically in Refs. 3, 17, 18.

Also, numerical analysis of Ref. 6, albeit carried out for 1D chiral systems, suggest that one-loop RG results accurately describe the critical properties of such type of transitions. Recently a value of $z = 1.49 \pm 0.02$ very close to the one-loop result $z = 3/2$ has been obtained numerically in Ref. 19. However, the same simulations found a value of $\nu = 1.47 \pm 0.03$ very different from the one-loop prediction $\nu = 1$. It has been argued in Ref. 20 that the one-loop result $z = 3/2$ for the dynamical critical exponent is exact and holds in all orders of the renormalisation, in contradiction with the analytical two-loop calculations of Ref. 11 predicting⁴⁰ $\nu = \left[-\varepsilon - \frac{\varepsilon^2}{8} + \dots\right]^{-1} \approx 1.14$ and $z = 1 - \frac{\varepsilon}{2} - \frac{3}{16}\varepsilon^2 + \dots \approx 1.31$. Similar analytical two-loop RG calculations for graphene²¹ and for related the Gross-Neveu model^{22–27}, with the results for the latter being well established in the high-energy literature, yield beta-functions inconsistent with those of Refs. 11 and 20.

In this paper we present an independent calculation of the critical exponents for the transition in a Weyl semimetal using a two-loop renormalisation group approach for Weyl fermions in $2 - \varepsilon$ dimensions and re-

solve controversies currently existing in the literature. We obtain beta functions consistent with those obtained for graphene in Ref. 21 and for Gross-Neveu model in Refs. 22–27, but in disagreement with the results of Refs. 11 and 20. We find the critical exponents to be

$$\nu = \left[-\varepsilon + \frac{\varepsilon^2}{2} + \dots \right]^{-1}, \quad (1)$$

$$z = 1 - \frac{\varepsilon}{2} - \frac{\varepsilon^2}{8} + \dots \quad (2)$$

For a 3D Weyl semimetal ($\varepsilon = -1$) Eqs. (1) and (2) give

$$\nu \approx 0.67, \quad z \approx 1.4. \quad (3)$$

We emphasise, however, that higher-loop corrections for $\varepsilon = -1$ will lead to deviations from these values obtained from an RG calculation controlled by small ε .

The critical density of states in a WSM with short-range-correlated disorder can be described in the supersymmetric representation²⁸ by a field theory with the action

$$\mathcal{L} = -i \int \Phi^\dagger \left[i\omega - \hat{\sigma} \mathbf{k} \right] \Phi \, d\mathbf{r} + \frac{1}{2} \kappa_0 \int (\Phi^\dagger \Phi)^2 d\mathbf{r}, \quad (4)$$

where $\Phi = (\chi \, s)^T$ is a vector consisting of an anti-commuting (fermionic) χ and commuting s (bosonic) components, $\omega > 0$ is the Matsubara frequency in the upper half-plane, $\hat{\sigma}$ is a vector of matrices generating a d -dimensional Clifford algebra ($\{\hat{\sigma}_\alpha, \hat{\sigma}_\beta\} = 2\delta_{\alpha\beta} \mathbb{1}$), $\mathbf{k} = -i\nabla$ is the momentum operator, and $\kappa_0 = \int \langle U(\mathbf{r})U(\mathbf{r}') \rangle_{\text{dis}} d\mathbf{r}'$ is the strength of the short-range-correlated random disorder potential under consideration. Equivalent field theories can be derived also in Keldysh²⁹ and replica³⁰ representations.

We emphasise, that we express the action (4) in terms of a positive Matsubara frequency ω , in contrast with the conventional real-frequency representation²⁸, in order to regularise integrals in the renormalisation scheme used below. Also, frequency ω in Eq. (4) plays the same role as the mass m in the related Gross-Neveu model^{23–25}. The density of states is determined by the retarded Green's function $G^R(E, \mathbf{r}, \mathbf{r}')$ that can be obtained from the action (4) using analytic continuation to real frequencies $i\omega \rightarrow E + i0$.

We note, that realistic materials always have an even number of Weyl nodes, due to the fermion doubling theorem³¹, and thus in general should be described by an action with an even number of Weyl fermion flavours. However, for sufficiently smooth disorder internodal scattering can be neglected, and the material is equivalent to an even number of copies of single-node WSMs described by the action (4).

In dimensions $d > 2$ this field theory leads to ultraviolet divergencies in physical observables and requires an appropriate RG treatment.

We study the behaviour of the system at frequency ω and at long length scales, $\mathbf{k} \rightarrow 0$, following the *minimal*

subtraction renormalisation scheme³². We use dimensional regularisation by computing observables in lower $d = 2 - \varepsilon$ dimensions (with small $\varepsilon > 0$) and then analytically continue renormalised observables to the higher dimensions of interest ($\varepsilon < 0$). The Lagrangian (4) in this scheme is separated into the effective Lagrangian \mathcal{L}_E of variables observable in the long-wave limit of interest and the counterterms:

$$\mathcal{L} = \mathcal{L}_E + \mathcal{L}_{\text{counter}}, \quad (5)$$

$$\mathcal{L}_E = -i \int \psi^\dagger \left(i\Omega - \hat{\sigma} \mathbf{k} \right) \psi \, d\mathbf{r} + \frac{1}{2} \kappa \int (\psi^\dagger \psi)^2 d\mathbf{r}, \quad (6)$$

where the energy scale Ω and the renormalised disorder strength κ are experimentally observable, and the counterterms $\mathcal{L}_{\text{counter}}$ cancel the divergent (in the powers of $1/\varepsilon$) contributions to physical observables that come from the Lagrangian (6).

The strength of disorder can be conveniently characterised by the dimensionless parameter⁵

$$\gamma = 2C_d \kappa \Omega^{-\varepsilon}, \quad (7)$$

where $C_d = 2^{1-d} \pi^{-\frac{d}{2}} / \Gamma(\frac{d}{2})$. For a given “bare” disorder strength κ_0 the renormalised dimensionless disorder strength γ and the characteristic energy Ω of the long-wave behaviour of disorder-averaged observables are related by the RG equation (see Appendix for a detailed derivation)

$$\frac{\partial \gamma}{\partial \ln \Omega} = -\varepsilon \gamma - \gamma^2 - \frac{1}{2} \gamma^3 + \dots \quad (8)$$

The dependence of Ω on the frequency ω is described by the RG equation

$$\left(\frac{\partial \ln \Omega}{\partial \ln \omega} \right)^{-1} = 1 + \frac{\gamma}{2} + \frac{\gamma^2}{8} + \dots \quad (9)$$

Our two-loop RG equations (8) and (9) are consistent with the previous studies of Weyl fermions in $d = 2 - \varepsilon$ dimensions: in the framework of Gross-Neveu model in Refs. 22–27 and of graphene in Ref. 21.

Eq. (8) shows that the dimensionless disorder strength grows or decreases depending on whether or not it exceeds a critical disorder strength

$$\gamma_c = -\varepsilon - \frac{\varepsilon^2}{2} + \dots \quad (10)$$

The existence of such a repulsive fixed point signals a transition, discussed in the literature^{1–5,10,11,17,19,20,33,34}, between a weak-disorder phase and a strong-disorder phase.

Using that near the transition $\frac{\partial \ln(\gamma - \gamma_c)}{\partial \ln \Omega} = -\nu^{-1}$ and Eq. (8) we obtain the correlation-length critical exponent (1). The divergence of ν in the $\varepsilon \rightarrow 0$ limit reflects the fact that $d = 2$ ($\varepsilon = 0$) is the lower critical dimension for this transition.

Our analysis predicts $\omega \propto \Omega^z$ at the critical disorder strength $\gamma = \gamma_c$. Eq. (9) then gives the dynamical critical exponent (2).

We note that for small $\varepsilon \ll 1$ the correlation-length exponent ν , Eq. (1), satisfies Harris criterion (Chayes inequality)^{35,36} $\nu \geq 2/d$. Because the correlation length $\xi \propto \Omega^{-1} \propto \omega^{-\frac{1}{z}}$ can be measured as a function of the energy ω for $\varkappa = \varkappa_c$ as well as a function of disorder strength $\xi \propto |\varkappa - \varkappa_c|^{-\nu}$ for $\omega = 0$, a similar criterion can be applied heuristically to the exponent $\tilde{\nu} = 1/z$, yielding $z \leq d/2$, consistent with our result Eq. (2).

In conclusion, we have presented a two-loop renormalisation-group analysis of the critical properties of the unconventional disorder-driven transition for Weyl fermions above two dimensions and found the correlation-length and dynamical critical exponents, Eqs. (1) and (2). The beta-functions that we obtain are consistent

with those for graphene and Gross-Neveu models studied previously in the literature⁴¹.

Acknowledgements. We appreciate useful discussions with A.W.W. Ludwig. Our work was supported by the Alexander von Humboldt Foundation through the Feodor Lynen Research Fellowship (SVS) and by the NSF grants DMR-1001240 (LR and SVS), DMR-1205303 (VG and SVS), PHY-1211914 (VG and SVS), and PHY-1125844 (SVS). LR also acknowledges support by the Simons Investigator award from the Simons Foundation.

Note added. After posting this paper on arXiv, the results of Refs. 20 and 11, contradicting our conclusions here, have been withdrawn by their authors; the claim of $z = 3/2$ being the exact dynamical exponent has been removed³⁷ by the authors of Ref. 20, while the results of Ref. 11 for the critical exponents have been retracted in erratum 38.

-
- ¹ E. Fradkin, Phys. Rev. B **33**, 3263 (1986).
 - ² E. Fradkin, Phys. Rev. B **33**, 3257 (1986).
 - ³ K. Kobayashi, T. Ohtsuki, K.-I. Imura, and I. F. Herbut, Phys. Rev. Lett. **112**, 016402 (2014).
 - ⁴ S. V. Syzranov, L. Radzihovsky, and V. Gurarie, Phys. Rev. Lett. **114**, 166601 (2015).
 - ⁵ S. V. Syzranov, V. Gurarie, and L. Radzihovsky, Phys. Rev. B **91**, 035133 (2015).
 - ⁶ M. Gärttner, S. V. Syzranov, A. M. Rey, V. Gurarie, and L. Radzihovsky, Phys. Rev. B **92**, 041406(R) (2015).
 - ⁷ S.-M. Huang, S.-Y. Xu, I. Belopolski, C.-C. Lee, G. Chang, B. Wang, N. Alidoust, G. Bian, M. Neupane, C. Zhang, et al., Nature Comm. **6**, 7373 (2015).
 - ⁸ S.-Y. Xu, I. Belopolski, N. Alidoust, M. Neupane, G. Bian, C. Zhang, R. Sankar, G. Chang, Z. Yuan, C.-C. Lee, et al., Science **349**, 613 (2015).
 - ⁹ B. Q. Lv, H. M. Weng, B. B. Fu, X. P. Wang, H. Miao, J. Ma, P. Richard, X. C. Huang, L. X. Zhao, G. F. Chen, et al., Phys. Rev. X **5**, 031013 (2015).
 - ¹⁰ P. Goswami and S. Chakravarty, Phys. Rev. Lett. **107**, 196803 (2011).
 - ¹¹ B. Roy and S. D. Sarma, Phys. Rev. B **90**, 241112(R) (2014).
 - ¹² S. Ryi and K. Nomura, Phys. Rev. B **85**, 155138 (2012).
 - ¹³ R. Shindou and S. Murakami, Phys. Rev. B **79**, 045321 (2009).
 - ¹⁴ Y. Ominato and M. Koshino, Phys. Rev. B **89**, 054202 (2014).
 - ¹⁵ I. L. Aleiner and K. B. Efetov, Phys. Rev. Lett. **97**, 236801 (2006).
 - ¹⁶ P. M. Ostrovsky, I. V. Gornyi, and A. D. Mirlin, Phys. Rev. B **74**, 235443 (2006).
 - ¹⁷ S. Liu, T. Ohtsuki, and R. Shindou (2015), arXiv:1507.02381.
 - ¹⁸ S. Bera, J. D. Sau, and B. Roy (2016), arXiv:1507.07551.
 - ¹⁹ B. Sbierski, E. J. Bergholtz, and P. W. Brouwer, Phys. Rev. B **92**, 115145 (2015).
 - ²⁰ J. H. Pixley, P. Goswami, and S. D. Sarma (2015), arXiv:1505.07938v2.
 - ²¹ A. Schuessler, P. M. Ostrovsky, I. V. Gornyi, and A. D. Mirlin, Phys. Rev. B **79**, 075405 (2009).
 - ²² W. Wetzels, Phys. Lett. **153B**, 297 (1985).
 - ²³ A. W. W. Ludwig, Nucl. Phys. B **285**, 97 (1987).
 - ²⁴ C. Luperini and P. Rossi, Ann. Phys. **212**, 371 (1991).
 - ²⁵ A. Bondi, G. Curci, G. Paffuti, and P. Rossi, Ann. Phys. **199**, 268 (1990).
 - ²⁶ N. D. Tracas and N. D. Vlachos, Phys. Lett. **236**, 333 (1990).
 - ²⁷ A. W. W. Ludwig and K. J. Wiese, Nucl. Phys. B **661**, 577 (2003).
 - ²⁸ K. B. Efetov, *Supersymmetry in Disorder and Chaos* (Cambridge University Press, New York, 1999).
 - ²⁹ A. Kamenev, *Field Theory of Non-Equilibrium Systems* (Cambridge Univ. Press, 2011).
 - ³⁰ D. Belitz and T. R. Kirkpatrick, Rev. Mod. Phys. **66**, 261 (1994).
 - ³¹ H. B. Nielsen and M. Ninomiya, Nuclear Physics B **185**, 20 (1981).
 - ³² M. E. Peskin and D. V. Schroeder, *An Introduction To Quantum Field Theory* (Addison-Wesley, 1975).
 - ³³ B. Sbierski, G. Pohl, E. J. Bergholtz, and P. W. Brouwer, Phys. Rev. Lett. **113**, 026602 (2014).
 - ³⁴ H. Shapourian and T. L. Hughes, Phys. Rev. B **93**, 075108 (2016).
 - ³⁵ J. T. Chayes, L. Chayes, D. S. Fisher, and T. Spencer, Phys. Rev. Lett. **57**, 2999 (1986).
 - ³⁶ A. B. Harris, J. Phys. C **7**, 3082 (1974).
 - ³⁷ J. H. Pixley, P. Goswami, and S. D. Sarma, Phys. Rev. B **93**, 085103 (2016).
 - ³⁸ B. Roy and S. D. Sarma (2016), arXiv:1602.03470.
 - ³⁹ A. A. Abrikosov, L. P. Gorkov, and I. E. Dzyaloshinski, *Methods of Quantum Field Theory in Statistical Physics* (Dover, New York, 1975).
 - ⁴⁰ We note that in Ref. 11 the parameter ε is defined as $\varepsilon = d - 2$, while our convention in this paper is $\varepsilon = 2 - d$.
 - ⁴¹ We note, that the sign of the coupling γ in the disordered problem under consideration is opposite to that of the respective models studied in high-energy literature for repulsively interacting fermions, which reflects in different signs of even-in- γ terms of beta-functions.

Appendix A: Renormalisation scheme

Disorder-averaged observables, e.g., the density of states or conductivity, calculated perturbatively in disorder strength using action (4) in dimensions $d > 2$ contain ultravioletly-divergent contributions that require an appropriate renormalisation-group treatment.

In this paper we use the minimal-subtraction renormalisation-group scheme³². The respective integrals in this scheme are evaluated in lower $d = 2 - \varepsilon$ dimensions ($\varepsilon > 0$), to ensure their ultraviolet convergence, making analytic continuation to higher dimensions ($\varepsilon < 0$) in the end of the calculation. Also, as we show below, the infrared convergence of momentum integrals is ensured by using Matsubara frequencies $i\Omega$ in place of real frequencies. The renormalisation procedure consists in calculating perturbative corrections to the disorder-free particle propagator

$$G(i\Omega, \mathbf{p}) = (i\Omega - \hat{\sigma}\mathbf{p})^{-1} = -\frac{i\Omega + \hat{\sigma}\mathbf{p}}{\Omega^2 + p^2} \quad (\text{A1})$$

and the coupling \varkappa in the Lagrangian (6) and adding counterterms $\mathcal{L}_{\text{counter}}$ to the Lagrangian in order to cancel divergent (in powers of $1/\varepsilon$) contributions. The renormalised quantities \varkappa and Ω can then be related to the “bare” \varkappa_0 and ω by comparing the initial Lagrangian (4) and the Lagrangian (5) expressed in the renormalised variables.

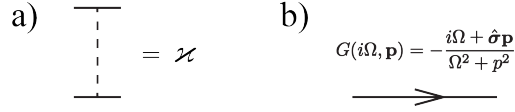


FIG. 1: Elements of the diagrammatic technique: a) impurity line and b) propagator.

Perturbative corrections to the propagator and disorder strength can be obtained straightforwardly using the Lagrangian (6). For convenience we utilise the conventional disorder-averaging diagrammatic technique³⁹, Fig. 1. The impurity line, Fig 1a, is a tensor product of two operators $\hat{\tau}_1 \otimes \hat{\tau}_2$ in the pseudospin subspaces that correspond to the two ends of the impurity line. Hereinafter scalar expressions for impurity lines are implied to be multiplied by $\mathbf{1} \otimes \mathbf{1}$.

Integrals in $d = 2 - \varepsilon$ dimensions

When evaluating diagrams below we use the following values of momentum integrals in dimension $2 - \varepsilon$:

$$\int_{\mathbf{p}} \frac{1}{p^2 + \Omega^2} = \frac{C_{2-\varepsilon}}{\varepsilon} \Omega^{-\varepsilon} + \mathcal{O}(\varepsilon), \quad (\text{A2a})$$

$$\int_{\mathbf{p}} \frac{1}{(p^2 + \Omega^2)^2} = \frac{1}{2} C_{2-\varepsilon} \Omega^{-2-\varepsilon} + \mathcal{O}(\varepsilon), \quad (\text{A2b})$$

$$\int_{\mathbf{p}} \frac{1}{(p^2 + \Omega^2)^3} = \frac{1}{4} C_{2-\varepsilon} \Omega^{-4-\varepsilon} + \mathcal{O}(\varepsilon), \quad (\text{A2c})$$

$$\int_{\mathbf{p}} \frac{1}{(i\Omega - \hat{\sigma}\mathbf{p})^2} = \left(\frac{1}{\varepsilon} - 1 \right) C_{2-\varepsilon} \Omega^{-\varepsilon} + \mathcal{O}(\varepsilon), \quad (\text{A2d})$$

$$\int_{\mathbf{p}} \frac{1}{(i\Omega - \hat{\sigma}\mathbf{p})^3} = -\frac{iC_{2-\varepsilon}}{2} \Omega^{-1-\varepsilon} + \mathcal{O}(\varepsilon), \quad (\text{A2e})$$

$$\int_{\mathbf{p}, \mathbf{q}} \frac{1}{(\Omega^2 + p^2)(\Omega^2 + q^2)[\Omega^2 + (\mathbf{p} + \mathbf{q})^2]} = \mathcal{O}(1), \quad (\text{A3a})$$

$$\int_{\mathbf{p}, \mathbf{q}} \frac{\mathbf{p}\mathbf{q}}{(\Omega^2 + p^2)(\Omega^2 + q^2)[\Omega^2 + (\mathbf{p} + \mathbf{q})^2]} = -\frac{1}{2} \left(\frac{C_{2-\varepsilon}}{\varepsilon} \Omega^{-\varepsilon} \right)^2 + \mathcal{O}(1), \quad (\text{A3b})$$

$$\int_{\mathbf{p}, \mathbf{q}} \frac{(\mathbf{p}\hat{\sigma})(\mathbf{q}\hat{\sigma})}{(\Omega^2 + p^2)(\Omega^2 + q^2)[\Omega^2 + (\mathbf{p} + \mathbf{q})^2]} = -\frac{1}{2} \left(\frac{C_{2-\varepsilon}}{\varepsilon} \Omega^{-\varepsilon} \right)^2 + \mathcal{O}(1), \quad (\text{A3c})$$

$$\int_{\mathbf{p}, \mathbf{q}} \frac{(\mathbf{p}\hat{\sigma})(\mathbf{q}\hat{\sigma})}{(\Omega^2 + p^2)^2(\Omega^2 + q^2)[\Omega^2 + (\mathbf{p} + \mathbf{q})^2]} = -\left(\frac{C_{2-\varepsilon}}{\varepsilon} \Omega^{-\varepsilon} \right)^2 \left(1 - \frac{\varepsilon}{2} \right) + \mathcal{O}(1), \quad (\text{A3d})$$

$$\int_{\mathbf{p}, \mathbf{q}} \frac{(\hat{\sigma}\mathbf{p})(\hat{\sigma}\mathbf{q})}{(\Omega^2 + p^2)^2(\Omega^2 + q^2)[\Omega^2 + (\mathbf{p} + \mathbf{q})^2]} = \mathcal{O}(1), \quad (\text{A3e})$$

$$\int_{\mathbf{p}, \mathbf{q}} \frac{\mathbf{p}\mathbf{q}}{(\Omega^2 + p^2)^2(\Omega^2 + q^2)[\Omega^2 + (\mathbf{p} + \mathbf{q})^2]} = \mathcal{O}(1), \quad (\text{A3f})$$

where the coefficient $C_{2-\varepsilon} = 2(4\pi)^{\frac{\varepsilon}{2}-1}/\Gamma(1 - \frac{\varepsilon}{2})$ is defined after Eq. (7), and $\int_{\mathbf{p}} \dots = \int d\mathbf{p}/(2\pi)^d \dots$

Detailed calculations of integrals (A2a)-(A2c) are presented, e.g., in Ref. 32. Integrals (A2d) and (A2e) can be reduced to similar integrals using $(i\Omega - \hat{\sigma}\mathbf{p})^{-1} = -(i\Omega + \hat{\sigma}\mathbf{p})/(\Omega^2 + p^2)$.

Integral (A3a) can be evaluated by introducing two Feynman parametrisations³²:

$$\begin{aligned} & \int_{\mathbf{p}, \mathbf{q}} \frac{1}{(\Omega^2 + p^2)(\Omega^2 + q^2)[\Omega^2 + (\mathbf{p} + \mathbf{q})^2]} = \int_{\mathbf{q}} \frac{1}{\Omega^2 + q^2} \int_0^1 du \int_{\mathbf{p}} \frac{1}{[\Omega^2 + (1-u)p^2 + u(\mathbf{p} + \mathbf{q})^2]^2} \\ &= \int_{\mathbf{q}} \frac{1}{\Omega^2 + q^2} \int_0^1 du \frac{C_d \Gamma(2 - \frac{d}{2}) \Gamma(\frac{d}{2})}{2\Gamma(2)} [\Omega^2 + u(1-u)q^2]^{\frac{d}{2}-2} \stackrel{\varepsilon \ll 1}{\approx} \frac{C_{2-\varepsilon}}{2} \int_0^1 du \int_{\mathbf{q}} \frac{1}{(\Omega^2 + q^2) [\Omega^2 + q^2 u(1-u)]^{2-\frac{d}{2}}} \\ &\approx \left(\frac{C_{2-\varepsilon}}{2} \right)^2 \int_0^1 \int_0^1 du dt \int_{\mathbf{q}} \frac{t^{1-\frac{d}{2}}}{[\Omega^2 + q^2 tu(1-u) + (1-t)q^2]^{3-\frac{d}{2}}} \approx \left(\frac{C_{2-\varepsilon}}{2} \right)^2 \Omega^{2-2\varepsilon} \int_0^1 \int_0^1 dt du \frac{t^{1-\frac{d}{2}}}{[tu(1-u) + 1-t]^{\frac{d}{2}}} = \mathcal{O}(1) \end{aligned} \quad (\text{A4})$$

Integral (A3b) can be reduced to the previous integrals by using that $\mathbf{p}\mathbf{q} = \frac{1}{2}(\mathbf{p} + \mathbf{q})^2 - \frac{1}{2}p^2 - \frac{1}{2}q^2$.

In order to evaluate integrals (A3c)-(A3f) we note that they are invariant under the interchange of \mathbf{p} and \mathbf{q} . They can thus be reduced to the previous integrals by replacing $(\mathbf{p}\hat{\sigma})(\mathbf{q}\hat{\sigma}) \rightarrow \frac{1}{2}[(\mathbf{p}\hat{\sigma})(\mathbf{q}\hat{\sigma}) + (\mathbf{q}\hat{\sigma})(\mathbf{p}\hat{\sigma})] = \frac{1}{2}(\mathbf{p} + \mathbf{q})^2 - \frac{1}{2}p^2 - \frac{1}{2}q^2$ or $\mathbf{p}\mathbf{q} \rightarrow \frac{1}{2}(\mathbf{p} + \mathbf{q})^2 - \frac{1}{2}p^2 - \frac{1}{2}q^2$.

Appendix B: One-loop renormalisations

One-loop renormalisation is mimicked by the diagrams in Fig. 2. In what follows expressions in square brackets is our convention for the values of the respective diagrams.

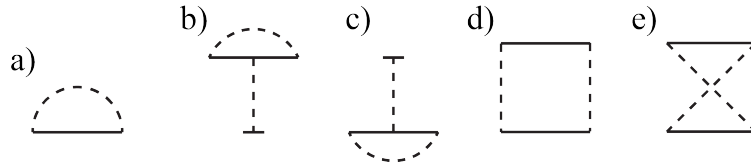


FIG. 2: Diagrams for the one-loop renormalisation: a) self-energy correction, b-e) vertex corrections.

Diagram 2a, the leading-order-in- \varkappa self-energy of the particles, is independent of the incoming and outgoing momenta and can be evaluated as

$$[2a] = \varkappa \int_{\mathbf{p}} (i\Omega - \hat{\sigma}\mathbf{p})^{-1} \stackrel{(\text{A2a})}{=} -i\Omega \varkappa \frac{C_{2-\varepsilon}}{\varepsilon} + \mathcal{O}(\varepsilon). \quad (\text{B1})$$

Diagrams 2b-2e mimic the corrections to the disorder strength \varkappa . Because we study the long-wavelength behaviour of the system (at finite frequency), these diagrams can be evaluated for zero incoming and outgoing momenta, integrating with respect to the intermediate momenta:

$$[2b] = [2c] = \varkappa^2 \int_{\mathbf{p}} (i\Omega - \hat{\sigma}\mathbf{p})^{-2} \stackrel{(A2d)}{=} \varkappa^2 \frac{C_{2-\varepsilon}}{\varepsilon} \Omega^{-\varepsilon} + \mathcal{O}(1), \quad (B2)$$

$$[2d] + [2e] = \varkappa^2 \int_{\mathbf{p}} \frac{1}{i\Omega - \hat{\sigma}\mathbf{p}} \otimes \frac{1}{i\Omega - \hat{\sigma}\mathbf{p}} + \varkappa^2 \int_{\mathbf{p}} \frac{1}{i\Omega - \hat{\sigma}\mathbf{p}} \otimes \frac{1}{i\Omega + \hat{\sigma}\mathbf{p}} = -\varkappa^2 \int_{\mathbf{p}} \frac{2\Omega^2}{(\Omega^2 + p^2)^2} = \mathcal{O}(1). \quad (B3)$$

To cancel the divergent in $1/\varepsilon$ corrections to the scale Ω and to the disorder strength \varkappa , given by Eqs. (B1) and (B2)-(B3) respectively, we add to the Lagrangian (6) the counterterm-Lagrangian

$$\mathcal{L}_{\text{counter}} = \int \delta^{(1)}\Omega \psi^\dagger \psi d\mathbf{r} + \frac{1}{2} \delta^{(1)}\varkappa \int (\psi^\dagger \psi)^2 d\mathbf{r}, \quad (B4)$$

$$\delta^{(1)}\varkappa = -2\varkappa^2 \frac{C_{2-\varepsilon}}{\varepsilon} \Omega^{-\varepsilon}, \quad (B5)$$

$$\delta^{(1)}\Omega = -\Omega \varkappa \frac{C_{2-\varepsilon}}{\varepsilon} \Omega^{-\varepsilon}. \quad (B6)$$

Eqs. (B5) and (B6) describe the one-loop renormalisation of the system parameters. We note, that there is no one-loop renormalisation of the particle velocity (the coefficient before $\hat{\sigma}\mathbf{k}$ in the Lagrangian).

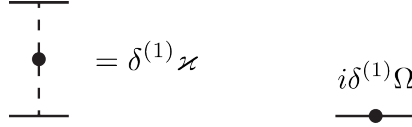


FIG. 3: Counterterms coming from the one-loop renormalisation.

In order to take into account these one-loop corrections when performing the two-loop renormalisation we introduce additional elements to the diagrammatic technique, Fig. 3.

Appendix C: Two-loop self-energy renormalisation

The two-loop contribution to the particle self-energy is given by the diagrams in Figs. 4 and 5. Diagram 4a depends on the external momentum \mathbf{k} , while the other diagrams are momentum-independent. The momentum dependency of the two-loop self-energy leads to the renormalisation of the particle velocity, in addition to the energy scale Ω .

1. Frequency renormalisation

In order to obtain the two-loop corrections to Ω it is sufficient to evaluate the diagrams in Figs. 4 and 5 for zero external momenta.

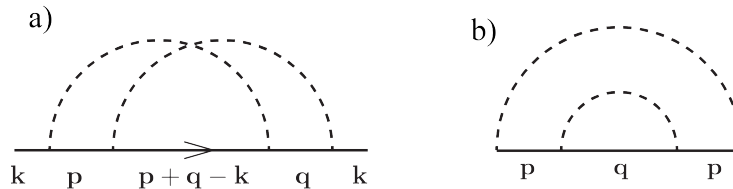


FIG. 4: Contributions to the renormalisation of the self-energy.

Diagrams 4a and 4b for $\mathbf{k} = 0$ are given by (in units \varkappa^2)

$$[4a] = - \int_{\mathbf{p}, \mathbf{q}} \frac{(i\Omega + \hat{\sigma}\mathbf{p}) [i\Omega + \hat{\sigma}(\mathbf{p} + \mathbf{q})] (i\Omega + \hat{\sigma}\mathbf{q})}{(\Omega^2 + p^2)[\Omega^2 + (\mathbf{p} + \mathbf{q})^2](\Omega^2 + q^2)} \quad (C1)$$

$$\stackrel{(A3a)}{=} -i\Omega \int_{\mathbf{p}, \mathbf{q}} \frac{(\mathbf{p}\hat{\sigma})(\mathbf{q}\hat{\sigma}) + (\mathbf{p}\hat{\sigma})(\mathbf{p}\hat{\sigma} + \mathbf{q}\hat{\sigma}) + (\mathbf{p}\hat{\sigma} + \mathbf{q}\hat{\sigma})(\mathbf{q}\hat{\sigma})}{(\Omega^2 + p^2)(\Omega^2 + q^2)[\Omega^2 + (\mathbf{p} + \mathbf{q})^2]} + \mathcal{O}(1) \stackrel{(A3c)}{=} -\frac{i\Omega}{2} \left(\frac{C_{2-\varepsilon}}{\varepsilon} \Omega^{-\varepsilon} \right)^2 + \mathcal{O}(1)$$

$$[4b] \stackrel{(A2a), (A2d)}{=} -i\Omega \left(\frac{C_{2-\varepsilon}}{\varepsilon} \Omega^{-\varepsilon} \right)^2 (1 - \varepsilon) + \mathcal{O}(1) \quad (C2)$$

Diagrams of the second order in the disorder strength \varkappa that contain the one-loop counterterms, Fig. 3, are shown in Fig. 5.



FIG. 5: Two-loop contributions to the self-energy that come from one-loop counterterms, Fig. 3.

$$[5a] = \varkappa \delta^{(1)} \varkappa \int_{\mathbf{p}} (i\Omega - \hat{\sigma}\mathbf{p})^{-2} \stackrel{(A2d), (B5)}{=} i\Omega \varkappa^2 \left(\frac{C_{2-\varepsilon}}{\varepsilon} \Omega^{-\varepsilon} \right)^2 (1 - \varepsilon) + \mathcal{O}(1) \quad (C3)$$

$$[5b] = 2i\Omega \varkappa^2 \left(\frac{C_{2-\varepsilon}}{\varepsilon} \Omega^{-\varepsilon} \right)^2 + \mathcal{O}(1). \quad (C4)$$

2. Velocity renormalisation

The velocity renormalisation is determined by the linear-in- \mathbf{k} contribution to the self-energy. In order to obtain it, we expand to the linear order the \mathbf{k} -dependent propagator in diagram 4a:

$$G_0(i\Omega, \mathbf{p} + \mathbf{q} - \mathbf{k}) \approx G_0(i\Omega, \mathbf{p} + \mathbf{q}) - G_0(i\Omega, \mathbf{p} + \mathbf{q})(\hat{\sigma}\mathbf{k})G_0(i\Omega, \mathbf{p} + \mathbf{q}). \quad (C5)$$

The diagram, corresponding to the linear-in- \mathbf{k} contribution, is shown in Fig. 6. In units \varkappa^2

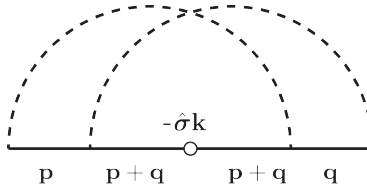


FIG. 6: Diagram for the velocity renormalisation.

$$[6] = - \int_{\mathbf{p}, \mathbf{q}} \frac{1}{i\Omega - \hat{\sigma}\mathbf{p}} \frac{1}{i\Omega - \hat{\sigma}(\mathbf{p} + \mathbf{q})} \hat{\sigma}\mathbf{k} \frac{1}{i\Omega - \hat{\sigma}(\mathbf{p} + \mathbf{q})} \frac{1}{i\Omega - \hat{\sigma}\mathbf{q}}$$

$$= - \int_{\mathbf{p}, \mathbf{q}} \frac{(i\Omega + \hat{\sigma}\mathbf{p})[i\Omega + \hat{\sigma}(\mathbf{p} + \mathbf{q})](\hat{\sigma}\mathbf{k})[i\Omega + \hat{\sigma}(\mathbf{p} + \mathbf{q})](i\Omega + \hat{\sigma}\mathbf{q})}{(\Omega^2 + p^2)[\Omega^2 + (\mathbf{p} + \mathbf{q})^2]^2(\Omega^2 + q^2)} \quad (C6)$$

Using that $(\hat{\sigma}\mathbf{p}_1)(\hat{\sigma}\mathbf{p}_2) + (\hat{\sigma}\mathbf{p}_2)(\hat{\sigma}\mathbf{p}_1) \equiv 2\mathbf{p}_1\mathbf{p}_2$, Eq. C6 gives

$$[6] = \int_{\mathbf{p}, \mathbf{q}} \frac{(i\Omega + \hat{\sigma}\mathbf{p})(\hat{\sigma}\mathbf{k})(i\Omega + \hat{\sigma}\mathbf{q})}{(\Omega^2 + p^2)[\Omega^2 + (\mathbf{p} + \mathbf{q})^2](\Omega^2 + q^2)} + I_1 \quad (C7)$$

where

$$I_1 = -2 \int_{\mathbf{p}, \mathbf{q}} \frac{(i\Omega + \hat{\sigma}\mathbf{p})[i\Omega + \hat{\sigma}(\mathbf{p} + \mathbf{q})](i\Omega + \hat{\sigma}\mathbf{q})}{(\Omega^2 + p^2)[\Omega^2 + (\mathbf{p} + \mathbf{q})^2]^2(\Omega^2 + q^2)} (\mathbf{p} + \mathbf{q})\mathbf{k} \quad (\text{C8})$$

Let us demonstrate that I_1 , Eq. (C8), does not contain $1/\varepsilon$ or $1/\varepsilon^2$ singularities. Replacing in the numerator $(i\Omega + \hat{\sigma}\mathbf{p})[i\Omega + \hat{\sigma}(\mathbf{p} + \mathbf{q})](i\Omega + \hat{\sigma}\mathbf{q}) \rightarrow p^2(\hat{\sigma}\mathbf{q}) + q^2(\hat{\sigma}\mathbf{p}) - 2\Omega^2\hat{\sigma}(\mathbf{p} + \mathbf{q})$ (as the other contributions vanish) and using (A3a) gives

$$I_1 = -2 \int_{\mathbf{p}, \mathbf{q}} \frac{p^2(\hat{\sigma}\mathbf{q}) + q^2(\hat{\sigma}\mathbf{p})}{(\Omega^2 + p^2)[\Omega^2 + (\mathbf{p} + \mathbf{q})^2]^2(\Omega^2 + q^2)} (\mathbf{p} + \mathbf{q})\mathbf{k} + \mathcal{O}(1) \quad (\text{C9})$$

Using that the integral in (C9) is invariant with respect to interchanging \mathbf{p} and \mathbf{q} and to changing signs of momentum components ($p_\alpha, q_\alpha \rightarrow -p_\alpha, -q_\alpha$), we replace $(\mathbf{q}\hat{\sigma}) \cdot [(\mathbf{p} + \mathbf{q})\mathbf{k}] \equiv \sum_{\alpha, \beta} \sigma_\alpha q_\alpha (p + q)_\beta k_\beta \rightarrow \sum_\alpha \sigma_\alpha q_\alpha (p + q)_\alpha k_\alpha \rightarrow \frac{1}{d} \mathbf{q}(\mathbf{p} + \mathbf{q}) \cdot (\hat{\sigma}\mathbf{k})$ and arrive at

$$\begin{aligned} I_1 &= -\frac{4}{d} \int_{\mathbf{p}, \mathbf{q}} \frac{p^2 \mathbf{q}(\mathbf{p} + \mathbf{q})}{(\Omega^2 + p^2)[\Omega^2 + (\mathbf{p} + \mathbf{q})^2]^2(\Omega^2 + q^2)} \hat{\sigma}\mathbf{k} \\ &= -\frac{4}{d} \int_{\mathbf{p}, \mathbf{q}} \frac{\mathbf{q}(\mathbf{p} + \mathbf{q})}{(\Omega^2 + q^2)[\Omega^2 + (\mathbf{p} + \mathbf{q})^2]} + \frac{4}{d} \Omega^2 \int_{\mathbf{p}, \mathbf{q}} \frac{\mathbf{q}(\mathbf{q} + \mathbf{p})}{(\Omega^2 + p^2)[\Omega^2 + (\mathbf{p} + \mathbf{q})^2]^2(\Omega^2 + q^2)} \stackrel{(\text{A3f})}{=} \mathcal{O}(1). \end{aligned} \quad (\text{C10})$$

Eqs. (C7), (C8), and (C10) give

$$\begin{aligned} [6] &= \int_{\mathbf{p}, \mathbf{q}} \frac{(\hat{\sigma}\mathbf{p})(\hat{\sigma}\mathbf{k})(\hat{\sigma}\mathbf{q})}{(\Omega^2 + p^2)(\Omega^2 + q^2)[\Omega^2 + (\mathbf{p} + \mathbf{q})^2]} + \mathcal{O}(1) \\ &= \left(\frac{2}{d} - 1\right) \int_{\mathbf{p}, \mathbf{q}} \frac{\mathbf{p}\mathbf{q}}{(\Omega^2 + p^2)(\Omega^2 + q^2)[\Omega^2 + (\mathbf{p} + \mathbf{q})^2]} \hat{\sigma}\mathbf{k} + \mathcal{O}(1) \stackrel{(\text{A3b})}{=} -\frac{1}{4\varepsilon} (C_{2-\varepsilon}\Omega^{-\varepsilon})^2 \hat{\sigma}\mathbf{k} + \mathcal{O}(1). \end{aligned} \quad (\text{C11})$$

Appendix D: Two-loop vertex renormalisation

The two-loop renormalisation of the disorder strength \varkappa corresponds to the diagrams in Figs. 7–13 (we show only topologically inequivalent diagrams). In what immediately follows we present a detailed calculation of each of these diagrams. For simplicity all expressions for the diagrams are given in units \varkappa^3 .

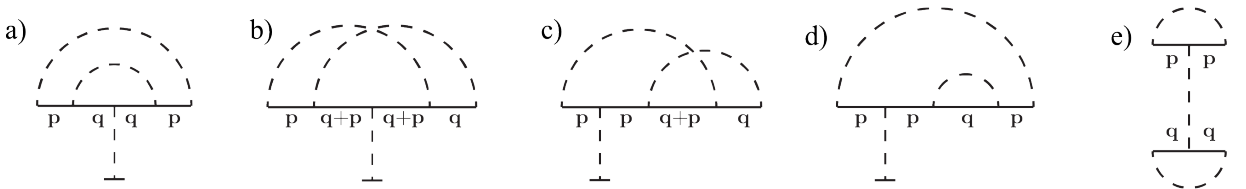


FIG. 7: Contributions to the two-loop renormalisation of the impurity line.

$$[7a] = \left[\int_{\mathbf{p}} \frac{1}{(i\Omega - \hat{\sigma}\mathbf{p})^2} \right]^2 \stackrel{(\text{A2a})}{=} (C_{2-\varepsilon}\Omega^{-\varepsilon}) \left(\frac{1}{\varepsilon^2} - \frac{2}{\varepsilon} \right) + \mathcal{O}(1) \quad (\text{D1})$$

$$\begin{aligned}
[7b] &= \int_{\mathbf{p}, \mathbf{q}} \frac{1}{i\Omega - \hat{\sigma}\mathbf{p}} \frac{1}{[i\Omega - \hat{\sigma}(\mathbf{p} + \mathbf{q})]^2} \frac{1}{i\Omega - \hat{\sigma}\mathbf{q}} = \int_{\mathbf{p}, \mathbf{q}} \frac{(i\Omega + \hat{\sigma}\mathbf{p})[i\Omega + \hat{\sigma}(\mathbf{p} + \mathbf{q})]^2(i\Omega + \hat{\sigma}\mathbf{q})}{(\Omega^2 + p^2)[\Omega^2 + (\mathbf{p} + \mathbf{q})^2]^2(\Omega^2 + q^2)} \\
&= \int_{\mathbf{p}, \mathbf{q}} \frac{(\hat{\sigma}\mathbf{p})(\hat{\sigma}\mathbf{q})(\mathbf{p} + \mathbf{q})^2}{(\Omega^2 + p^2)[\Omega^2 + (\mathbf{p} + \mathbf{q})^2]^2(\Omega^2 + q^2)} - \Omega^2 \int_{\mathbf{p}, \mathbf{q}} \frac{2(\hat{\sigma}\mathbf{p})(\hat{\sigma}\mathbf{p} + \hat{\sigma}\mathbf{q}) + 2(\hat{\sigma}\mathbf{p} + \hat{\sigma}\mathbf{q})(\hat{\sigma}\mathbf{q}) + (\hat{\sigma}\mathbf{p})(\hat{\sigma}\mathbf{q})}{(\Omega^2 + p^2)[\Omega^2 + (\mathbf{p} + \mathbf{q})^2]^2(\Omega^2 + q^2)} + \mathcal{O}(1) \\
&\stackrel{(A3a)}{=} \int_{\mathbf{p}, \mathbf{q}} \frac{(\hat{\sigma}\mathbf{p})(\hat{\sigma}\mathbf{q})}{(\Omega^2 + p^2)[\Omega^2 + (\mathbf{p} + \mathbf{q})^2](\Omega^2 + q^2)} - 2\Omega^2 \int_{\mathbf{p}, \mathbf{q}} \frac{(\hat{\sigma}\mathbf{p})(\hat{\sigma}\mathbf{q})}{(\Omega^2 + p^2)[\Omega^2 + (\mathbf{p} + \mathbf{q})^2]^2(\Omega^2 + q^2)} + \mathcal{O}(1) \\
&= \int_{\mathbf{p}, \mathbf{q}} \frac{(\hat{\sigma}\mathbf{p})(\hat{\sigma}\mathbf{q})}{(\Omega^2 + p^2)[\Omega^2 + (\mathbf{p} + \mathbf{q})^2](\Omega^2 + q^2)} - \Omega^2 \int_{\mathbf{p}, \mathbf{q}} \frac{(\mathbf{p} + \mathbf{q})^2 - p^2 - q^2}{(\Omega^2 + p^2)[\Omega^2 + (\mathbf{p} + \mathbf{q})^2]^2(\Omega^2 + q^2)} + \mathcal{O}(1) \\
&\stackrel{(A3c), (A3b), (A2b), (A2d)}{=} -\frac{1}{2}\mathcal{K}^3(C_{2-\varepsilon}\Omega^{-\varepsilon})^2 \left(\frac{1}{\varepsilon^2} - \frac{2}{\varepsilon} \right) + \mathcal{O}(1), \tag{D2}
\end{aligned}$$

$$\begin{aligned}
[7c] &= \int_{\mathbf{p}, \mathbf{q}} \frac{1}{(i\Omega - \hat{\sigma}\mathbf{p})^2} \frac{1}{i\Omega - \hat{\sigma}(\mathbf{p} + \mathbf{q})} \frac{1}{i\Omega - \hat{\sigma}\mathbf{q}} \\
&\stackrel{\mathbf{p}+\mathbf{q} \rightarrow \mathbf{p}, \mathbf{q} \rightarrow -\mathbf{q}}{=} \int_{\mathbf{p}, \mathbf{q}} \frac{[i\Omega + \hat{\sigma}(\mathbf{p} + \mathbf{q})]^2}{[\Omega^2 + (\mathbf{p} + \mathbf{q})^2]} \frac{i\Omega + \hat{\sigma}\mathbf{p}}{\Omega^2 + p^2} \frac{i\Omega - \hat{\sigma}\mathbf{q}}{\Omega^2 + q^2} \\
&= - \int_{\mathbf{p}, \mathbf{q}} \frac{(\mathbf{p} + \mathbf{q})^2(\hat{\sigma}\mathbf{p})(\hat{\sigma}\mathbf{q})}{(\Omega^2 + p^2)[\Omega^2 + (\mathbf{p} + \mathbf{q})^2]^2(\Omega^2 + q^2)} \\
&\quad - \Omega^2 \int_{\mathbf{p}, \mathbf{q}} \frac{2(\hat{\sigma}\mathbf{p} + \hat{\sigma}\mathbf{q})(\hat{\sigma}\mathbf{p}) + 2(\hat{\sigma}\mathbf{p} + \hat{\sigma}\mathbf{q})(\hat{\sigma}\mathbf{q}) - (\hat{\sigma}\mathbf{p})(\hat{\sigma}\mathbf{q})}{(\Omega^2 + p^2)[\Omega^2 + (\mathbf{p} + \mathbf{q})^2]^2(\Omega^2 + q^2)} + \mathcal{O}(1) \\
&= -[7b] + \mathcal{O}(1) = \frac{1}{2}\mathcal{K}^3(C_{2-\varepsilon}\Omega^{-\varepsilon})^2 \left(\frac{1}{\varepsilon^2} - \frac{2}{\varepsilon} \right) + \mathcal{O}(1) \tag{D3}
\end{aligned}$$

$$[7d] = \int_{\mathbf{p}} \left(\frac{1}{i\Omega - \hat{\sigma}\mathbf{p}} \right)^3 \int_{\mathbf{q}} \frac{1}{i\Omega - \hat{\sigma}\mathbf{p}} \stackrel{(A2a), (A2e)}{=} -\frac{1}{2\varepsilon} (C_{2-\varepsilon}\Omega^{-\varepsilon})^2 + \mathcal{O}(1) \tag{D4}$$

$$[7e] = \int_{\mathbf{p}} \frac{1}{(i\Omega - \hat{\sigma}\mathbf{p})^2} \otimes \int_{\mathbf{q}} \frac{1}{(i\Omega - \hat{\sigma}\mathbf{q})^2} \stackrel{(A2d)}{=} (C_{2-\varepsilon}\Omega^{-\varepsilon})^2 \left(\frac{1}{\varepsilon^2} - \frac{2}{\varepsilon} \right) + \mathcal{O}(1) \tag{D5}$$

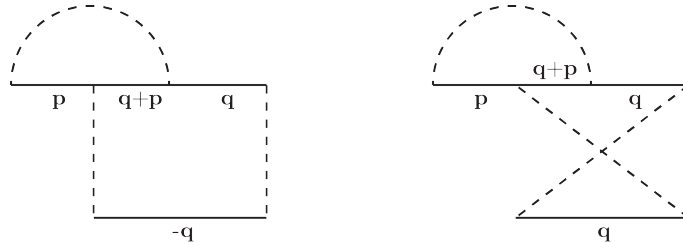


FIG. 8: Contribution to the two-loop renormalisation of the impurity line.

$$\begin{aligned}
[8] &= \int_{\mathbf{p}, \mathbf{q}} \frac{1}{i\Omega - \hat{\sigma}\mathbf{p}} \frac{1}{i\Omega - \hat{\sigma}(\mathbf{p} + \mathbf{q})} \frac{1}{i\Omega - \hat{\sigma}\mathbf{q}} \otimes \left(\frac{1}{i\Omega - \hat{\sigma}\mathbf{q}} + \frac{1}{i\Omega + \hat{\sigma}\mathbf{q}} \right) \\
&= 2i\Omega \int \frac{(i\Omega + \hat{\sigma}\mathbf{p})[i\Omega + \hat{\sigma}(\mathbf{p} + \mathbf{q})](i\Omega + \hat{\sigma}\mathbf{q})}{(\Omega^2 + p^2)[\Omega^2 + (\mathbf{p} + \mathbf{q})^2](\Omega^2 + q^2)^2} = -2\Omega^2 \int_{\mathbf{p}, \mathbf{q}} \frac{(\hat{\sigma}\mathbf{p})(\hat{\sigma}\mathbf{q}) + (\mathbf{p} + \mathbf{q})^2}{(\Omega^2 + p^2)[\Omega^2 + (\mathbf{p} + \mathbf{q})^2](\Omega^2 + q^2)^2} + \mathcal{O}(1) \\
&= -\Omega^2 \int_{\mathbf{p}, \mathbf{q}} \frac{3(\mathbf{p} + \mathbf{q})^2 - p^2 - q^2}{(\Omega^2 + p^2)[\Omega^2 + (\mathbf{p} + \mathbf{q})^2](\Omega^2 + q^2)^2} \\
&= -3\Omega^2 \int_{\mathbf{p}, \mathbf{q}} \frac{1}{(\Omega^2 + p^2)(\Omega^2 + q^2)^2} + \Omega^2 \int_{\mathbf{p}, \mathbf{q}} \frac{1}{[\Omega^2 + (\mathbf{q} + \mathbf{p})^2](\Omega^2 + q^2)^2} + \mathcal{O}(1) \\
&\stackrel{(A2a), (A2b)}{=} -\frac{1}{\varepsilon} (C_{2-\varepsilon}\Omega^{-\varepsilon})^2 + \mathcal{O}(1) \quad (D6)
\end{aligned}$$

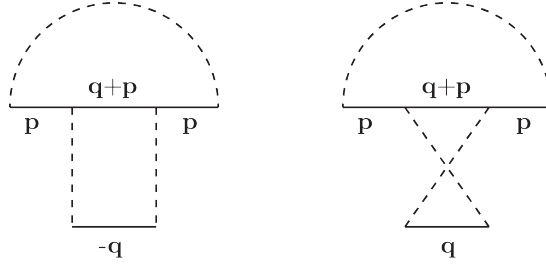


FIG. 9: Contribution to the two-loop renormalisation of the impurity line.

$$\begin{aligned}
[9] &= \int_{\mathbf{p}, \mathbf{q}} \frac{1}{i\Omega - \hat{\sigma}\mathbf{p}} \frac{1}{i\Omega - \hat{\sigma}(\mathbf{p} + \mathbf{q})} \frac{1}{i\Omega - \hat{\sigma}\mathbf{p}} \otimes \left(\frac{1}{i\Omega - \hat{\sigma}\mathbf{q}} + \frac{1}{i\Omega + \hat{\sigma}\mathbf{q}} \right) \\
&= 2i\Omega \int \frac{(i\Omega + \hat{\sigma}\mathbf{p})[i\Omega + \hat{\sigma}(\mathbf{p} + \mathbf{q})](i\Omega + \hat{\sigma}\mathbf{p})}{(\Omega^2 + p^2)^2[\Omega^2 + (\mathbf{p} + \mathbf{q})^2](\Omega^2 + q^2)} = -2\Omega^2 \int_{\mathbf{p}, \mathbf{q}} \frac{(\mathbf{p}^2 + \mathbf{q}^2) - p^2 - q^2}{(\Omega^2 + p^2)^2[\Omega^2 + (\mathbf{p} + \mathbf{q})^2](\Omega^2 + q^2)} + \mathcal{O}(1) \\
&\stackrel{(A3a)}{=} -2\Omega^2 \int_{\mathbf{p}, \mathbf{q}} \frac{1}{(\Omega^2 + p^2)^2(\Omega^2 + q^2)} + 2\Omega^2 \int_{\mathbf{p}, \mathbf{q}} \frac{1}{(\Omega^2 + p^2)^2[\Omega^2 + (\mathbf{p} + \mathbf{q})^2]} + \mathcal{O}(1) = \mathcal{O}(1) \quad (D7)
\end{aligned}$$

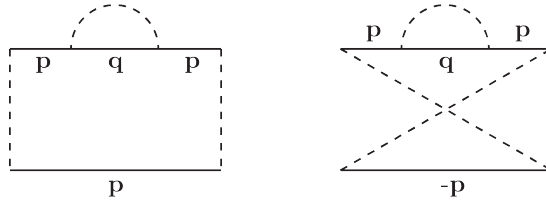


FIG. 10: Contribution to the two-loop renormalisation of the impurity line.

$$\begin{aligned}
[10] &= \int_{\mathbf{p}, \mathbf{q}} \frac{1}{i\Omega - \hat{\sigma}\mathbf{p}} \frac{1}{i\Omega - \hat{\sigma}\mathbf{q}} \frac{1}{i\Omega - \hat{\sigma}\mathbf{p}} \otimes \left(\frac{1}{i\Omega - \hat{\sigma}\mathbf{p}} + \frac{1}{i\Omega + \hat{\sigma}\mathbf{p}} \right) \\
&\stackrel{(A2a)}{=} \left[-i\Omega \frac{C_{2-\varepsilon}}{\varepsilon} \Omega^{-\varepsilon} + \mathcal{O}(\varepsilon) \right] \cdot 2i\Omega \int_{\mathbf{p}} \frac{(2i\Omega + \hat{\sigma}\mathbf{p})^2}{(\Omega^2 + p^2)^3} = 2\Omega^2 \left[\frac{C_{2-\varepsilon}}{\varepsilon} + \mathcal{O}(\varepsilon) \right] \cdot \left[\int_{\mathbf{p}} \frac{1}{(\Omega^2 + p^2)^2} - 2\Omega^2 \int_{\mathbf{p}} \frac{1}{(\Omega^2 + p^2)^3} \right] \\
&\stackrel{(A2b), (A2b)}{=} \frac{1}{\varepsilon} \cdot \mathcal{O}(\varepsilon) = \mathcal{O}(1) \quad (D8)
\end{aligned}$$

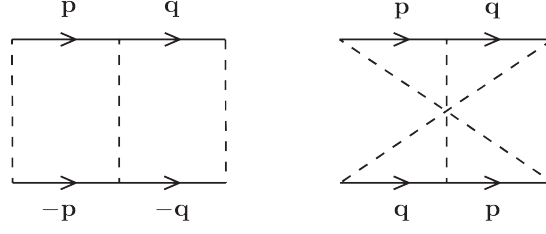


FIG. 11: Contribution to the two-loop renormalisation of the impurity line.

The sum of the two diagrams in Fig. 11 is given by

$$\begin{aligned}
 [11] &= \int_{\mathbf{p}, \mathbf{q}} \frac{1}{i\Omega - \hat{\sigma}\mathbf{p}} \frac{1}{i\Omega - \hat{\sigma}\mathbf{q}} \otimes \frac{1}{i\Omega + \hat{\sigma}\mathbf{p}} \frac{1}{i\Omega + \hat{\sigma}\mathbf{q}} + \int_{\mathbf{p}, \mathbf{q}} \frac{1}{i\Omega - \hat{\sigma}\mathbf{p}} \frac{1}{i\Omega - \hat{\sigma}\mathbf{q}} \otimes \frac{1}{i\Omega - \hat{\sigma}\mathbf{q}} \frac{1}{i\Omega - \hat{\sigma}\mathbf{p}} \\
 &= \int_{\mathbf{p}, \mathbf{q}} \frac{(i\Omega + \hat{\sigma}\mathbf{p})(i\Omega + \hat{\sigma}\mathbf{q}) \otimes [-2\Omega^2 + (\hat{\sigma}\mathbf{p})(\hat{\sigma}\mathbf{q}) + (\hat{\sigma}\mathbf{q})(\hat{\sigma}\mathbf{p})]}{(\Omega^2 + p^2)^2(\Omega^2 + q^2)^2} = 2 \int_{\mathbf{p}, \mathbf{q}} \frac{[-\Omega^2 + (\hat{\sigma}\mathbf{p})(\hat{\sigma}\mathbf{q})] \otimes (-\Omega^2 + \mathbf{p}\mathbf{q})}{(\Omega^2 + p^2)^2(\Omega^2 + q^2)^2} \\
 &= 2 \int_{\mathbf{p}, \mathbf{q}} \frac{(\hat{\sigma}\mathbf{p})(\hat{\sigma}\mathbf{q}) \otimes \mathbf{p}\mathbf{q}}{(\Omega^2 + p^2)^2(\Omega^2 + q^2)^2} + \mathcal{O}(1) \quad (\text{D9})
 \end{aligned}$$

Using that in the tensor product $(\hat{\sigma}\mathbf{p})(\hat{\sigma}\mathbf{q}) \otimes \mathbf{p}\mathbf{q} = \sum_{\alpha, \beta, \gamma} \sigma_\alpha p_\alpha \sigma_\beta q_\beta \otimes p_\gamma q_\gamma$ only the terms with $\alpha = \beta = \gamma$ contribute to the integral (D9) we replace $(\hat{\sigma}\mathbf{p})(\hat{\sigma}\mathbf{q}) \otimes \mathbf{p}\mathbf{q} \rightarrow \sum_\alpha p_\alpha^2 q_\alpha^2 \rightarrow \frac{1}{d} p^2 q^2$:

$$\begin{aligned}
 [11] &= \frac{2}{d} \left[\int_{\mathbf{p}} \frac{p^2}{(\Omega^2 + p^2)^2} \right]^2 = \frac{2}{d} \left[\int_{\mathbf{p}} \frac{1}{\Omega^2 + p^2} - \Omega^2 \int_{\mathbf{p}} \frac{1}{(\Omega^2 + p^2)^2} \right]^2 \\
 &= \frac{2}{2 - \varepsilon} \left[\frac{1}{\varepsilon} C_{2-\varepsilon} \Omega^{-\varepsilon} - \frac{1}{2} C_{2-\varepsilon} \Omega^{-\varepsilon} + \mathcal{O}(\varepsilon) \right]^2 = \left(\frac{1}{\varepsilon^2} - \frac{1}{2\varepsilon} \right) (C_{2-\varepsilon} \Omega^{-\varepsilon})^2 + \mathcal{O}(1). \quad (\text{D10})
 \end{aligned}$$

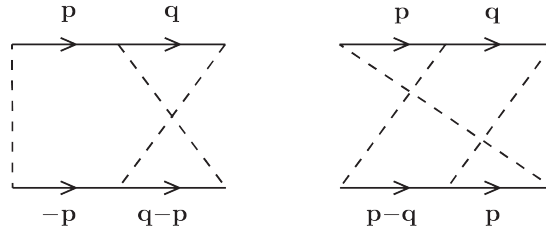


FIG. 12: Contribution to the two-loop renormalisation of the impurity line.

$$\begin{aligned}
[12] &= \int_{\mathbf{p}, \mathbf{q}} \frac{1}{i\Omega - \hat{\sigma}\mathbf{p}} \frac{1}{i\Omega - \hat{\sigma}\mathbf{q}} \otimes \frac{1}{i\Omega + \hat{\sigma}\mathbf{p}} \frac{1}{i\Omega + \hat{\sigma}(\mathbf{p} - \mathbf{q})} + \int_{\mathbf{p}, \mathbf{q}} \frac{1}{i\Omega - \hat{\sigma}\mathbf{p}} \frac{1}{i\Omega - \hat{\sigma}\mathbf{q}} \otimes \frac{1}{i\Omega - \hat{\sigma}(\mathbf{p} - \mathbf{q})} \frac{1}{i\Omega - \hat{\sigma}\mathbf{p}} \\
&= \int_{\mathbf{p}, \mathbf{q}} \frac{(i\Omega + \hat{\sigma}\mathbf{p})(i\Omega + \hat{\sigma}\mathbf{q}) \otimes [-2\Omega^2 + (\hat{\sigma}\mathbf{p})(\hat{\sigma}\mathbf{p} - \hat{\sigma}\mathbf{q}) + (\hat{\sigma}\mathbf{p} - \hat{\sigma}\mathbf{q})(\hat{\sigma}\mathbf{p})]}{(\Omega^2 + p^2)^2(\Omega^2 + q^2)[\Omega^2 + (\mathbf{p} - \mathbf{q})^2]} \\
&= 2 \int_{\mathbf{p}, \mathbf{q}} \frac{(i\Omega + \hat{\sigma}\mathbf{p})(i\Omega + \hat{\sigma}\mathbf{q}) \otimes [-\Omega^2 + \mathbf{p}(\mathbf{p} - \mathbf{q})]}{(\Omega^2 + p^2)^2(\Omega^2 + q^2)[\Omega^2 + (\mathbf{p} - \mathbf{q})^2]} = 2 \int_{\mathbf{p}, \mathbf{q}} \frac{[-\Omega^2 + (\hat{\sigma}\mathbf{p})(\hat{\sigma}\mathbf{q})][-\Omega^2 + \mathbf{p}(\mathbf{p} - \mathbf{q})]}{(\Omega^2 + p^2)^2(\Omega^2 + q^2)[\Omega^2 + (\mathbf{p} - \mathbf{q})^2]} \\
&= 2 \int_{\mathbf{p}, \mathbf{q}} \frac{(\hat{\sigma}\mathbf{p})(\hat{\sigma}\mathbf{q}) \otimes \mathbf{p}(\mathbf{p} - \mathbf{q})}{(\Omega^2 + p^2)^2(\Omega^2 + q^2)[\Omega^2 + (\mathbf{p} - \mathbf{q})^2]} - 2\Omega^2 \int_{\mathbf{p}, \mathbf{q}} \frac{(\hat{\sigma}\mathbf{p})(\hat{\sigma}\mathbf{q}) \otimes \mathbf{1}}{(\Omega^2 + p^2)^2(\Omega^2 + q^2)[\Omega^2 + (\mathbf{p} - \mathbf{q})^2]} \\
&\quad - 2\Omega^2 \int_{\mathbf{p}, \mathbf{q}} \frac{\mathbf{1} \otimes \mathbf{p}(\mathbf{p} - \mathbf{q})}{(\Omega^2 + p^2)^2(\Omega^2 + q^2)[\Omega^2 + (\mathbf{p} - \mathbf{q})^2]} + \mathcal{O}(1) \stackrel{(A3e), (A3f)}{=} \int_{\mathbf{p}, \mathbf{q}} \frac{(\hat{\sigma}\mathbf{p})(\hat{\sigma}\mathbf{q}) \otimes [p^2 + (\mathbf{p} - \mathbf{q})^2 - q^2]}{(\Omega^2 + p^2)^2(\Omega^2 + q^2)[\Omega^2 + (\mathbf{p} - \mathbf{q})^2]} + \mathcal{O}(1) \\
&= \int_{\mathbf{p}, \mathbf{q}} \frac{(\hat{\sigma}\mathbf{p})(\hat{\sigma}\mathbf{q}) \otimes \mathbf{1}}{(\Omega^2 + p^2)(\Omega^2 + q^2)[\Omega^2 + (\mathbf{p} - \mathbf{q})^2]} - \int_{\mathbf{p}, \mathbf{q}} \frac{(\hat{\sigma}\mathbf{p})(\hat{\sigma}\mathbf{q}) \otimes \mathbf{1}}{(\Omega^2 + p^2)^2[\Omega^2 + (\mathbf{p} - \mathbf{q})^2]} \\
&\quad - \Omega^2 \int_{\mathbf{p}, \mathbf{q}} \frac{(\hat{\sigma}\mathbf{p})(\hat{\sigma}\mathbf{q})}{(\Omega^2 + p^2)^2(\Omega^2 + q^2)[\Omega^2 + (\mathbf{p} - \mathbf{q})^2]} + \mathcal{O}(1) \\
&\stackrel{(A3c), (A3d)}{=} \frac{1}{2} \left(\frac{C_{2-\varepsilon}}{\varepsilon} \Omega^{-\varepsilon} \right)^2 - \left(\frac{C_{2-\varepsilon}}{\varepsilon} \Omega^{-\varepsilon} \right)^2 \left(1 - \frac{\varepsilon}{2} \right) + \mathcal{O}(1) = -\frac{1}{2} (C_{2-\varepsilon} \Omega^{-\varepsilon})^2 \left(\frac{1}{\varepsilon^2} + \frac{1}{\varepsilon} \right) + \mathcal{O}(1)
\end{aligned} \tag{D11}$$

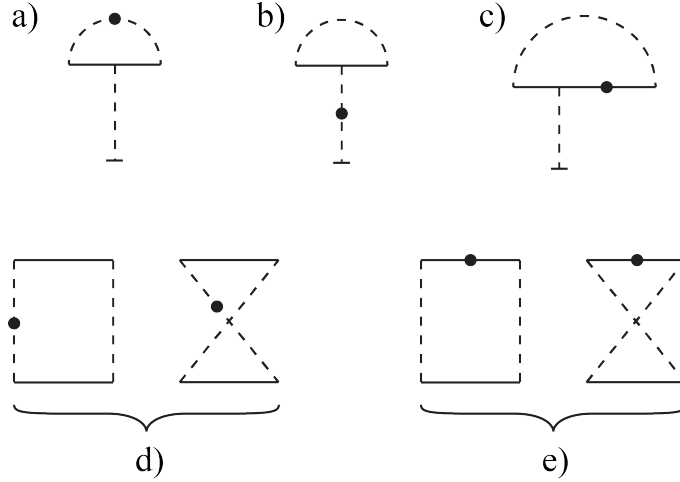


FIG. 13: Diagrams for the two-loop renormalisation with one-loop counterterms.

Diagrams for the two-loop renormalisation that contain the one-loop counterterms, Fig. 3, are shown in Fig. 13. Diagram 13c can be evaluated straightforwardly using Eq. (A2e), and the other diagrams—similarly to the corresponding one-loop diagrams in Fig. 2:

$$[13a] = [13b] = -2\kappa^3 (C_{2-\varepsilon} \Omega^{-\varepsilon})^2 \left(\frac{1}{\varepsilon^2} - \frac{1}{\varepsilon} \right) + \mathcal{O}(1), \tag{D12}$$

$$[13c] = \frac{1}{2} \kappa^3 (C_{2-\varepsilon} \Omega^{-\varepsilon})^2 / \varepsilon + \mathcal{O}(1), \tag{D13}$$

$$[13d] = 2\kappa^3 (C_{2-\varepsilon} \Omega^{-\varepsilon})^2 / \varepsilon + \mathcal{O}(1), \tag{D14}$$

$$[13e] = \mathcal{O}(1). \tag{D15}$$

Appendix E: RG equations

In the previous sections we calculated in two loops perturbative corrections to observable couplings Ω , \varkappa , and the quasiparticle velocity (coefficient before $\hat{\sigma}\hat{\mathbf{k}}$) that come from the action (6) and contain divergent contributions $\propto 1/\varepsilon$ and $1/\varepsilon^2$. In order to cancel these divergencies, following the minimal subtraction scheme³², we add to the action (6) the counterterm Lagrangian

$$\mathcal{L}_{\text{counter}} = -i \int \psi^\dagger \left[\delta(i\Omega) - \delta(\hat{\sigma}\hat{\mathbf{k}}) \right] \psi \, d\mathbf{r} + \frac{1}{2} \delta \varkappa \int (\psi^\dagger \psi)^2 \, d\mathbf{r}, \quad (\text{E1})$$

where

$$\delta(i\Omega) = [2a] + [4a]_{\mathbf{k}=0} + [4b] + [5a] + [5b] = i\Omega \left[-\frac{1}{\varepsilon} \varkappa C_{2-\varepsilon} \Omega^{-\varepsilon} + \frac{3}{2} \frac{1}{\varepsilon^2} (\varkappa C_{2-\varepsilon} \Omega^{-\varepsilon})^2 \right], \quad (\text{E2})$$

$$\delta(\hat{\sigma}\hat{\mathbf{k}}) = -[6] = \frac{1}{4\varepsilon} (\varkappa C_{2-\varepsilon} \Omega^{-\varepsilon})^2 \hat{\sigma}\hat{\mathbf{k}} \quad (\text{E3})$$

$$\begin{aligned} \delta \varkappa = & -[2b - e] - 2 \times [7a] - 2 \times [7b] - 4 \times [7c] - 4 \times [7d] - [7e] - 4 \times [8] - 2 \times [9] - 2 \times [10] - [11] - 2 \times [12] \\ & - 2 \times [13a] - 2 \times [13b] - 4 \times [13c] - 2 \times [13d] - 2 \times [13e] = \varkappa \left[-\frac{2}{\varepsilon} \varkappa C_{2-\varepsilon} \Omega^{-\varepsilon} - \left(-\frac{4}{\varepsilon^2} + \frac{1}{2\varepsilon} \right) (\varkappa C_{2-\varepsilon} \Omega^{-\varepsilon})^2 \right] \end{aligned} \quad (\text{E4})$$

where we kept only the terms divergent at $\varepsilon \rightarrow 0$ and took into account the numbers of topologically equivalent diagrams.

Introducing dimensionless disorder strength, Eq. (7), the full Lagrangian (5) of the system can be rewritten in terms of the observable variables \varkappa and Ω as

$$\mathcal{L} = -i \int \psi^\dagger \left[i\Omega \left(1 - \frac{\gamma}{2\varepsilon} + \frac{3}{8} \frac{\gamma^2}{\varepsilon^2} \right) - \hat{\sigma}\hat{\mathbf{k}} \left(1 + \frac{\gamma^2}{16\varepsilon} \right) \right] \psi \, d\mathbf{r} - \frac{\gamma \Omega^\varepsilon}{4C_{2-\varepsilon}} \left(1 - \frac{\gamma}{\varepsilon} - \frac{\gamma^2}{8\varepsilon} + \frac{\gamma^2}{\varepsilon^2} \right) \int (\psi^\dagger \psi)^2 \, d\mathbf{r}. \quad (\text{E5})$$

The renormalised observables ψ , γ , and Ω can be related to the “bare” Φ , \varkappa_0 and ω by comparing the Lagrangian (E5) with the “bare” one, Eq. (4):

$$Z = 1 + \frac{\gamma^2}{16\varepsilon}, \quad (\text{E6})$$

$$\varkappa_0 = \frac{\Omega^\varepsilon}{2C_{2-\varepsilon}} \gamma \left(1 - \frac{\gamma}{\varepsilon} + \frac{\gamma^2}{\varepsilon^2} - \frac{\gamma^2}{4\varepsilon} \right), \quad (\text{E7})$$

$$\omega = \Omega \left(1 - \frac{\gamma}{2\varepsilon} + \frac{3\gamma^2}{8\varepsilon^2} - \frac{\gamma^2}{16\varepsilon} \right), \quad (\text{E8})$$

where Z describes the rescaling of the particle wavefunctions: $\psi = \Phi/Z^{\frac{1}{2}}$.

The energy scale Ω sets the characteristic momentum of long-wavelength behaviour of the system. In order to obtain the RG flow of the renormalised disorder strength γ as a function of Ω for a given bare disorder strength \varkappa_0 , we require

$$\frac{\partial \varkappa_0}{\partial \ln \Omega} = 0, \quad (\text{E9})$$

which, together with Eq. (E7), gives the RG equation (8).

RG equation (9) follows straightforwardly from Eq. (E8).